Solvent Effects on the Barrier to C−N Bond Rotation in *N*,*N*-Dimethylaminoacrylonitrile: Modeling by Reaction Field Theory and by Monte Carlo Simulations

Paul R. Rablen,* Shoshannah A. Pearlman, and Deborah A. Miller

Contribution from the Department of Chemistry, Swarthmore College, 500 College Ave., Swarthmore, Pennsylvania 19081-1397

Received July 1, 1998

Abstract: Solvents are known experimentally to influence strongly the barrier to rotation about the conjugated C−N bond of *N*,*N*-dimethylaminoacrylonitrile (DMAAN). The barrier increases with overall solvent polarity, but solvent hydrogen-bond donor ability does not have a measurable effect. Two solvation models were explored in an attempt to reproduce the experimental data and obtain insight into the causes of the observed solvent effects. Calculations based on the isodensity polarizable continuum model (IPCM) encoded in Gaussian 94, a representative dielectric continuum-based procedure, yielded fair agreement for aprotic, nonhalogenated, nonaromatic solvents. The model predicts a linear correlation with the Onsager dielectric function, $(\epsilon - 1)/(2\epsilon + 1)$, which was observed experimentally for this set of solvents. However, the model underestimated the magnitude of the solvent dependence by approximately 30%. As a representative example of an approach based on the use of explicit solvent molecules, Monte Carlo simulations were carried out with Jorgensen's BOSS package. The simulations strongly underestimated the influence of cyclohexane, consistent with earlier Monte Carlo studies of amides in nonpolar solvents. The simulations also underestimated the solvent effects in acetonitrile and methanol, but reproduced the experimental data in water quite closely. Radial distribution functions from the water simulations showed that the lack of an explicit hydrogen-bonding contribution to the solvent effect resulted from a generally weak set of interactions between the cyano nitrogen and the nearest neighbor water molecule. Furthermore, these interactions changed very little as rotation about the amino C−N bond took place. The simulations suggested that hydrogen bonding to DMAAN is far more pronounced and variable in methanol, but the experimental data did not support this conclusion. None of the simulations showed significant hydrogen bonding to the amino lone pair. The possibility is raised that some of the apparent inconsistencies in the calculations might result from the inappropriate treatment of the transition state as a species for which the solution environment is equilibrated.

Introduction

Modeling of the solution environment represents an important and growing area of interest within computational chemistry. The utility of ab initio molecular orbital calculations is by now well established, but an understanding of the influence of the solvent is required to make the connection to the solution environment that is frequently of primary experimental interest. Reliable models of solvation establish this link in a quantitative fashion. Continuum models represent a simple and popular approach to describing the solution environment and have been explored extensively. They enjoy the advantage of an intrinsic computational economy, and yet have proved quite successful in a variety of applications.[1,10,12−14] Statistical mechanical simulations with ensembles of explicit solvent molecules are widely used to describe organic and biological solutes in dilute solution, particularly in water and in situations where specific

(1) For reviews of continuum solvation models, see: (a) Tomasi, J.; Persico, M. *Chem. Rev.* **1994**, *94*, 2027−2094. (b) Cramer, C. J.; Truhlar, D. G. *Rev. Comput. Chem.* **1990**, *6*, 1−72.

(2) (a) Mennucci, B.; Tomasi, J. *J. Chem. Phys.* **1997**, *106*, 5151−5158 and references therein. (b) Miertus, S.; Scrocco, E.; Tomasi, J. *Chem. Phys.* **1981**, *55*, 117−129. (c) Tomasi, J.; Bonaccorsi, R.; Cammi, R.; Valle, F. O. J. *J. Mol. Struct.* **1991**, *234*, 401.

(3) Foresman, J.; Keith, T. A.; Wiberg, K. B.; Snoonian, J.; Frisch, M. *J. Phys. Chem.* **1996**, *100*, 16098−16104.

(4) Kollman, P. A. *Chem. Rev.* **1993**, *93*, 2395−2417.

(5) (a) Jorgensen, W. L. *Acc. Chem. Res.* **1989**, *22*, 184−189. (b) Jorgensen, W. L. *J. Phys. Chem.* **1983**, *87*, 5304−5314.

(6) (a) Gao, J.; Freindorf, M. *J. Phys. Chem. A* **1997**, *101*, 3182−3188. (b) Gao, J. L. *Acc. Chem. Res.* **1996**, *29*, 298−305. (c) Gao, J.; Alhambra, C. *J. Am. Chem. Soc.* **1997**, *119*, 2962−2963.

(7) Marten, B.; Kim, K.; Cortis, C.; Friesner, R. A.; Murphy, R. B.; Ringnalda, M. N.; Sitkoff, D.; Honig, B. *J. Phys. Chem.* **1996**, *100*, 11775−11788.

(8) Chen, W.; Gordon, M. S. *J. Chem. Phys.* **1996**, *105*, 11081−11090.

(9) Bader, J. S.; Cortis, C. M.; Berne, B. J. *J. Chem. Phys.* **1997**, *106*, 2372−2387.

(10) (a) Giesen, D. J.; Gu, M. Z.; Cramer, C. J.; Truhlar, D. G. *J. Org. Chem.* **1996**, *61*, 8720−8721. (b) Chambers, C. C.; Hawkins, G. D.; Cramer, C. J.; Truhlar, D. G. *J. Phys. Chem.* **1996**, *100*, 16385−16398.

(11) Hummer, G.; Pratt, L. R.; García, A. E. *J. Am. Chem. Soc.* **1997**, *119*, 8523−8527.

(12) Still, W. C.; Tempczyk, A.; Hawley, R. C.; Hendrickson, T. *J. Am. Chem. Soc.* **1990**, *112*, 6127−6129.

(13) Truong, T. N.; Stefanovich, E. V. *J. Phys. Chem.* **1995**, *99*, 14700−14706. Truong, T. N.; Truong, T.-T. T.; Stefanovich, E. V. *J. Phys. Chem.* **1997**, *107*, 11881-1889.

(14) (a) Edinger, S. R.; Cortis, C.; Shenkin, P. S.; Friesner, R. A. *J. Phys. Chem. B* **1997**, *101*, 1190−1197. (b) Luo, H. Q.; Tucker, S. C. *J. Phys. Chem. B* **1997**, *101*, 1063−1071. (c) Alagona, G.; Ghio, C.; Nagy, P. I.; Durant, G. J. *J. Phys. Chem.* **1994**, *98*, 5422−5430. (d) Best, S. A.; Merz, K. M.; Reynolds, C. H. *J. Phys. Chem. B* **1997**, *101*, 10479−10487. (e) Harris, N. J.; Ohwada, T.; Lammertsa, K. *J. Comput. Chem.* **1998**, *19*, 250−257. (f) Elcock, A. H.; McCammon, J. A. *J. Phys. Chem. B* **1997**, *101*, 9624−9634.

10.1021/ja9823058 CCC: $18.00
Published on Web 12/19/1998

solute−solvent interactions are of paramount importance.[4,5,1515] Calculations of this sort are increasingly used to help understand experimental observations in such areas as host−guest chemistry[16] and protein folding.[17] Once such a model has been validated, it can be used to derive molecular-level detail about the behavior of a system that would be very difficult to obtain in any other way. This sort of precise structural information can facilitate understanding in much the same way as a crystal structure.

However, all these models require calibration and testing against experimental data. Conformational isomerizations represent some of the simplest and structurally most well-defined reactions known, and consequently are particularly well suited to this task. In principle, both conformational equilibria and rates of conformational change can be studied. A number of studies of the solvent dependence of conformational equilibria have been published,[18,19] although a need still exists for additional systematic data concerning a wide variety of systems in a broad selection of solvents. However, relatively few systematic studies of solvent effects on conformational isomerization rates have been performed.[20−24] The experimentally accessible rates of isomerization yield information about the relative stabilization of the equilibrium structure and the transition state structure for the isomerization reaction, and thus allow an examination of how well various models reproduce the solvation energies of these species.

Detailed kinetic studies have been carried out previously regarding amide bond rotation, which is known to be retarded by polar solvents.[21,22,25] Particularly detailed data[22,25] as well as corresponding calculations[22,26,27] are available for *N*,*N*-dimethylformamide (DMF) (**1a**) and *N*,*N*-dimethylacetamide (DMA) (**1b**). Each of these amides has two possible transition states for rotation, since the nitrogen becomes pyramidal in the transition state, and the lone pair can point in a direction either syn or anti to the carbonyl oxygen. These transition states are shown and labeled in Scheme 1. With DMA, the transition state structure with the lone pair anti to the carbonyl (DMA TS #1, **2b**) is favored in the gas phase and in aprotic solvents, but calculations suggest that the "syn" structure (**3b**) might be competitive or even preferred in aqueous solution.[26] With DMF, on the other hand, the "syn" structure (DMF TS #2, **3a**) is predicted by calculation to be favored under all circumstances, although the "anti" structure (**2a**) is only slightly higher in energy in the gas phase and in nonpolar solvents. The gas-phase barriers have been measured experimentally by NMR spectroscopy,[28] and the agreement with high-level ab initio predictions (e.g., using Pople's G-2 procedure[29]) is within 0.5 kcal/mol.[22]

Scheme 1

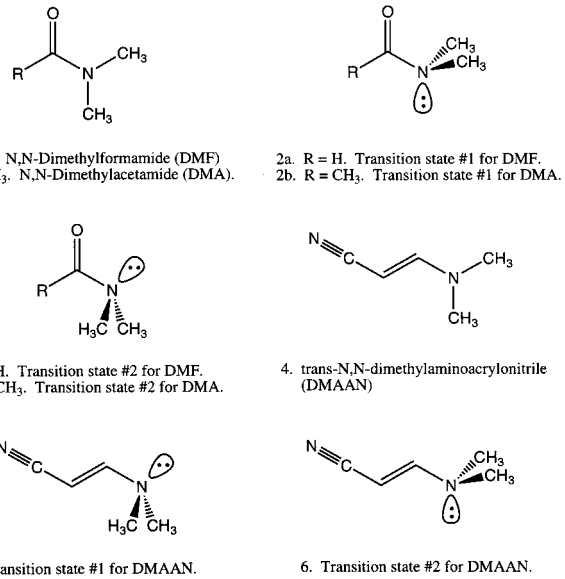

The transition state structures for DMF and DMA are predicted to have lower dipole moments than the equilibrium structures, although the difference is larger for the case of DMA, where the "anti" transition state is preferred. Simple electrostatic considerations thus predict that a more polar environment should raise the barrier to bond rotation, and that the effect should be larger for DMA than for DMF. Experimental measurements have shown this to be the case, and in fact the magnitude of the solvent effect agrees very well with the predictions of a polarizable continuum reaction field model, at least for certain "well-behaved" aprotic solvents that lack second-row elements and aromatic rings.[22] According to this model, the magnitude of the solvent effect should have a very nearly linear dependence on the Onsager dielectric function, defined as $(\epsilon - 1)/(2\epsilon + 1)$, where ϵ is the dielectric constant.

Furthermore, protic solvents, such as methanol and water, increase the observed barriers to rotation substantially more than their dielectric constants alone would "predict". This effect has been attributed to hydrogen bonding by the solvent, and is in accord with the calculated effect of adding a single water molecule to the equilibrium and transition state structures of

(15) Allen, M. P.; Tildesley, D. J. *Computer Simulations of Liquids*; Clarendon Press: Oxford, UK, 1987.

(16) (a) Denti, T. Z. M.; van Gunsteren, W. F.; Diederich, F. *J. Am. Chem. Soc.* **1996**, *118*, 6044−6051. (b) Jorgensen, W. L.; Nguyen, T. B. *Proc. Natl. Acad. Sci. U.S.A.* **1993**, *90*, 1194−1200.

(17) (a) Tirado-Rives, J.; Jorgensen, W. L. *Biochemistry* **1997**, *36*, 7313−7329. (b) Humphreys, D. D.; Friesner, R. A.; Berne, B. J. *J. Phys. Chem.* **1995**, *99*, 10674−10685. (c) Schiffer, C. A.; Dötsch, V.; Wütrich, K.; van Gunsteren, W. F. *Biochemistry* **1995**, *34*, 15057−15067.

(18) (a) Perrin, C. L.; Fabian, M. A.; Rivero, I. A. *J. Am. Chem. Soc.* **1998**, *120*, 1044−1047. (b) Nagy, P. I.; Takács-Novák, K. *J. Am. Chem. Soc.* **1997**, *119*, 4999−5006. (c) Wong, M. W.; Wiberg, K. B.; Frisch, M. J. *J. Am. Chem. Soc.* **1992**, *114*, 1645−1652. (d) Wiberg, K. B.; Wong, M. W. *J. Am. Chem. Soc.* **1993**, *115*, 1078−1084. (e) Wiberg, K. B.; Marquez, M. M. *J. Am. Chem. Soc.* **1994**, *116*, 2197−2198. (f) Jorgensen, W. L.; Morales de Tirado, P. I.; Severance, D. L. *J. Am. Chem. Soc.* **1994**, *116*, 2199−2200.

(19) (a) Wiberg, K. B.; Keith, T. A.; Frisch, M. J.; Murcko, M. *J. Phys. Chem.* **1995**, *99*, 9072−9079. (b) Foresman, J. B.; Keith, T. A.; Wiberg, K. B.; Snoonian, J.; Frisch, M. J. *J. Phys. Chem.* **1996**, *100*, 16098−16104.

(20) Reichardt, C. *Solvents and Solvent Effects in Organic Chemistry*, 2nd ed.; VCH Publishers: Germany, 1988.

(21) (a) Stewart, W. E.; Siddall, T. H., III *Chem. Rev.* **1970**, *70*, 517−551 and references therein. (b) Drakenberg, T.; Dahlqvist, K. J.; Forsen, S. *J. Phys. Chem.* **1972**, *76*, 2178−2183.

(22) Wiberg, K. B.; Rablen, P. R.; Rush, D. J.; Keith, T. A. *J. Am. Chem. Soc.* **1995**, *117*, 4261−4270.

(23) (a) Cox, C.; Young, V. G., Jr.; Lectka, T. *J. Am. Chem. Soc.* **1997**, *119*, 2307−2308. (b) Cox, C.; Ferraris, D.; Murthy, N. N.; Lectka, T. *J. Am. Chem. Soc.* **1996**, *118*, 5332−5333.

(24) Chiara, J. L.; Gómez-Sánchez, A.; Bellanato, J. *J. Chem. Soc., Perkin Trans. 2* **1992**, 787−798.

(25) Suarez, C.; LeMaster, C. B.; LeMaster, C. L.; Tafazzoli, M.; True, N. S. *J. Phys. Chem.* **1990**, *94*, 6679−6683.

(26) Duffy, E. M.; Severance, D. L.; Jorgensen, W. L. *J. Am. Chem. Soc.* **1992**, *114*, 7535−7542.

(27) Gao, J. *J. Am. Chem. Soc.* **1993**, *115*, 2930−2935. Gao, J. *Proc. Indian Acad. Sci.* **1994**, *106*, 507.

(28) (a) Ross, B. D.; True, N. S. *J. Am. Chem. Soc.* **1984**, *106*, 2451−2452. Cf. LeMaster, C. B.; True, N. S. *J. Phys. Chem.* **1989**, *93*, 1307−1311. (b) Ross, B. D.; True, N. S.; Matson, G. B. *J. Phys. Chem.* **1984**, *88*, 2675−2678. (c) Feigel, M. *J. Chem. Soc. Chem. Commun.* **1980**, 456−457. (d) Feigel, M. *J. Phys. Chem.* **1983**, *87*, 3054−3058. The $\Delta G^{\ddagger}$ values reported in (c) and (d) were based on a transmission coefficient of 1.0, and were recalculated using 0.5 to be consistent with the values given in (a) and (b) and the values reported in the current work.

(29) (a) Curtiss, L. A.; Raghavachari, K.; Trucks, G. W.; Pople, J. A. *J. Chem. Phys.* **1991**, *94*, 7221−7230. (b) Curtiss, L. A.; Carpenter, J. E.; Raghavachari, K.; Pople, J. A. *J. Chem. Phys.* **1992**, *96*, 9030−9034.

DMF.[22] While the continuum reaction field model is unable to treat this situation correctly, Jorgensen and co-workers have successfully described the effect of aqueous solvation on the DMA rotational barrier using Monte Carlo statistical mechanical simulations.[26] The simulations reproduce the experimentally observed difference in solvent effect between water and carbon tetrachloride, but seem to underestimate the absolute magnitude of the solvent effects by about 1.5 kcal/mol. Gao and co-workers have achieved similar results for DMF using a combined quantum mechanical and molecular mechanical simulation methodology,[27] predicting a solvent effect of 1.0 kcal/mol in water, which somewhat underestimates the experimental value of 2.8 kcal/mol.[22]

In the preceding paper, we have reported an experimental study of the solvent effects on rotation about the conjugated C−N bond of *N*,*N*-dimethylaminoacrylonitrile (DMAAN) along with gas-phase ab initio calculations.[30] The equilibrium structure and two possible transition state structures are depicted in Scheme 1. Both theory and experimental inference indicate that the barrier to rotation is approximately 9.3 kcal/mol in the gas phase, and calculations show that the second transition state structure **6** is strongly favored over the alternative structure **5**. In analogy to the amides,[22] solvent polarity was observed to increase the barrier to rotation. In contrast to the case of amides, however, hydrogen bond donor ability of the solvent was found to have little effect on the observed barrier. Here we have carried out calculations using two procedures for computing solvation energies both to test the models and to gain insight into the nature of the solvent effects in this system. The isodensity polarizable continuum model (IPCM), which has met with some success in application to the amides,[22] was taken as a representative continuum-based model, and was used to investigate the nonspecific effect of solvent polarity on the isomerization reaction. Monte Carlo statistical mechanical simulations[26] in water and several other solvents were then carried out in an attempt to reproduce the experimental data for protic solvents and to understand the reason hydrogen bond donor ability has little effect on the rotational barrier.

Results

Reaction Field Theory. Reaction field theory, first developed by Onsager and Kirkwood,[31] provides a simple model for calculating the electrostatic component of solvation energies. The model treats the solvent as a continuum characterized only by a static dielectric constant and a cavity in which the solute is situated. The electrical moments of the solute cause the continuum to become polarized, and the resulting electrostatic interactions between the solute and the continuum lead to stabilization. The model neglects terms in the solvation energy associated with formation of the cavity. However, for conformational isomerization reactions the cavity is unlikely to change much over the course of the reaction, and so this shortcoming is of little consequence for the current application.

Reaction field theory has been adapted for use with ab initio MO calculations in the form of self-consistent reaction field (SCRF) theory, so-called because the reaction field component of the energy is incorporated directly into the Hamiltonian and the molecular wave function is thus optimized in a manner that includes the solvation energy.[1,2,32−35] The most recent version of the Gaussian ab initio molecular orbital package incorporates several versions of reaction field theory, including the isodensity polarizable continuum model (IPCM) and self-consistent IPCM (SCIPCM) implementations.[3,19,22,36] In both cases, the molecular wave function is used to define the solvent−solute interface, i.e., the surface at which the dielectric constant abruptly drops to zero. Previous work has shown that the 0.0004 electron per cubic Bohr electron density surface serves as an appropriate definition of the boundary, and yields satisfactory agreement with experiment for a variety of systems.[19,22] The choice of 0.0004 as the isodensity contour enjoys the additional advantage that the enclosed volumes correlate closely with experimental molecular volumes.[19a] The IPCM model uses the gas-phase molecular wave function to define the boundary surface, while with the SCIPCM model the surface is determined self-consistently in the presence of the polarizable medium.

Table 1. Calculated Solvent Effect on the Barrier to Rotation about the Conjugated C−N Bond in DMAAN Using the IPCM Model (kcal/mol)[a]

	$\Delta\Delta G^{\ddagger}(298)$[b]		
method	TS1	TS2	total
HF/6-31G*	2.64	2.72	2.72
Becke3LYP/6-31G*	2.88	2.89	2.89
Becke3LYP/6-311++G**	2.89	3.02	3.02
MP2/6-31G*	2.24	2.87	2.87
MP2/6-311++G**	2.23	2.88	2.88

[a] Calculated with the dielectric constant ϵ set to 78 and the molecular surface defined as the 0.0004 electrons per cubic Bohr surface. [b] Calculated using the gas-phase MP2/6-31G* optimized geometries.

The SCRF approach has proven effective for treating the effects of nonassociating solvents on the rotational barriers of amides,[22] and so it was of interest to apply the same procedure to the case of DMAAN. The results of a series of calculations with the IPCM model are presented in Table 1. Calculations carried out with the closely related SCIPCM model generally gave very similar results. However, the SCIPCM procedure encountered convergence problems in some cases, and so we have focused on the IPCM results instead. Calculations at the Hartree−Fock level, at the MP2 level, and with Becke3LYP hybrid density functional theory with either the 6-31G* or 6-311++G** basis set all furnished very similar results that only varied within a narrow range of about 10%. For instance, the predicted solvent effect with $\epsilon = 78$ ranges from 2.72 to 3.02 kcal/mol depending on the theoretical model. The MP2/6-311++G** numbers probably constitute the single most reliable set. As illustrated in Figure 1 and in Table 2, the dependence of the calculated solvent effect on the Onsager dielectric function, $(\epsilon - 1)/(2\epsilon + 1)$, is almost perfectly linear. Consequently, simple interpolation can be used to determine the IPCM predicted solvent effect for any value of the dielectric constant. Table 3 makes direct comparisons between the experimental and calculated solvent effects by using just such an interpolation procedure to obtain a predicted solvent effect in each particular solvent that was studied experimentally.

(30) Previous paper in this issue: Rablen, P. R.; Miller, D. A.; Bullock, V. R.; Hutchinson, P. H.; Gorman, J. A. *J. Am. Chem. Soc.* **1999**, *121*, 218−226.

(31) Onsager, L. *J. Am. Chem. Soc.* **1936**, *58*, 1486−1493. Kirkwood, J. G. *J. Chem. Phys.* **1934**, *2*, 351−361. Born, M. *Z. Phys.* **1920**, *1*, 45−48.

(32) (a) Tapia, O.; Goscinski, O. *Mol. Phys.* **1975**, *29*, 1653−1661. (b) Rivail, J. L.; Terryn, B.; Ruiz-López, M. F. *J. Mol. Struct.: THEOCHEM* **1985**, *120*, 387.

(33) Cf.: Wong, M. W.; Frisch, M. J.; Wiberg, K. B. *J. Am. Chem. Soc.* **1991**, *113*, 4776−4782. Wong, M. W.; Wiberg, K. B.; Frisch, M. J. *J. Chem. Phys.* **1991**, *95*, 8991−8998.

(34) Rinaldi, D.; Ruiz-Lopez, M. F.; Rivail, J.-L. *J. Chem. Phys.* **1983**, *78*, 834−838.

(35) Miertus, S.; Scrocco, E.; Tomasi, J. *Chem. Phys*, **1981**, *55*, 117. Tomasi, J.; Bonaccorsi, R.; Cammi, R.; Valle, F. O. J. *J. Mol. Struct.* **1991**, *234*, 401.

(36) Clifford, S.; Keith, T. A.; Frisch, M. J. To be submitted for publication.

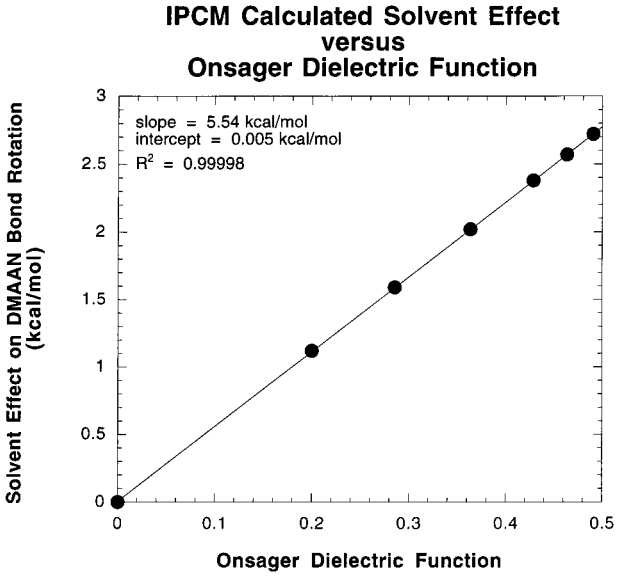

Figure 1. Relationship between the Onsager dielectric function $(\epsilon - 1)/(2\epsilon + 1)$ and the solvent effect on the DMAAN barrier calculated via the IPCM method. Best fit line: solvent effect (kcal/mol) = 5.54∗-$(\epsilon - 1)/(2\epsilon + 1)$ + 0.005; $r^2 = 0.99998$.

Table 2. Calculated Dependence of the Solvent Effect on the Dielectric Constant[a]

	$\Delta\Delta G^{\ddagger}(298)$[c]		
ϵ[b]	TS1	TS2	total
2.0	1.12	1.12	1.12
3.0	1.59	1.59	1.59
5.0	2.00	2.02	2.02
10.0	2.33	2.38	2.38
20.0	2.50	2.57	2.57
78.0	2.64	2.72	2.72

[a] Using the IPCM model, with the molecular surface defined as the 0.0004 electrons per cubic Bohr surface. Energies in kcal/mol. [b] Dielectric constant. [c] Calculated at the HF/6-31G* level, using the gas-phase optimized geometries.

Table 3. Calculated Solvent Effects on the Barrier to Rotation about the Conjugated C−N Bond in *N*,*N*-Dimethylaminoacrylonitrile (kcal/mol)

		$\Delta\Delta G^{\ddagger}(298)$[a]			
solvent	ϵ[b]	TS1	TS2	total	exp
methylcyclohexane	2.0	0.91	1.17	1.17	1.7
dibutyl ether	3.1	1.33	1.71	1.71	2.24
acetone	20.6	2.11	2.73	2.73	3.50
methanol	32.0	2.17	2.80	2.80	3.66
acetonitrile	37.5	2.18	2.82	2.82	4.04
water	78.0	2.23	2.88	2.88	≤3.7

[a] Derived via interpolation of MP2/6-311++G** IPCM calculations for $\epsilon = 78$ (Table 1), using the linear dependence of the model on the Onsager dielectric function $(\epsilon - 1)/(2\epsilon + 1)$. [b] Dielectric constant. Source: Reichardt, C. *Solvents and Solvent Effects in Organic Chemistry*, 2nd ed.; VCH: New York, 1990.

Table 4 shows the effects of changing the isodensity contour level used in the IPCM model. The value of 0.0004 electrons per cubic Bohr has been recommended,[19] and has worked well previously for amides,[22] but additional calculations were performed with 0.0001, 0.0002, 0.001, and 0.002 electrons per cubic Bohr. The final results are surprisingly insensitive to this empirical parameter, so that even quite large variations lead only to small changes in the calculated solvent effect. This stability lends further credibility to the predictions of the model.

Table 4. Calculated Dependence of the Solvent Effect on the Electron Density Contour[a]

	$\Delta\Delta G^{\ddagger}(298)$[c]		
contour[b]	TS1	TS2	total
0.0001	2.04	2.21	2.21
0.0002	2.32	2.46	2.46
0.0004	2.64	2.72	2.72
0.0010	2.93	3.01	3.01
0.0020	2.10	3.04	3.03

[a] Using the IPCM model, with the dielectic constant set to 78.0; energies in kcal/mol. [b] Contour of electron density, in electrons per cubic Bohr, used for the IPCM model. [c] Calculated at the HF/6-31G* level, using the gas-phase optimized geometries.

Statistical Mechanical Simulations. Monte Carlo statistical mechanical simulations were carried out in an attempt to reproduce available experimental data and to gain insight into the specific intermolecular interactions responsible for the observed solvent effects. Standard free-energy perturbation methodology[5,15] was used as implemented in the BOSS program[37] to determine the change in the free energy of solvation upon transformation of the equilibrium structure to either of the two possible transition state structures. Our approach follows that used by Duffy, Severance, and Jorgensen in their investigation of DMA,[26] except that we have employed charges fit to the HF/6-31G* molecular electrostatic potential and an MP2/6-31+G* optimized geometry to describe the solute. Previous experience has shown that the HF/6-31G* procedure yields molecular charge distributions that are somewhat too strongly polarized in the gas phase and that are consequently quite appropriate for solution calculations.[38] Duffy et al. used a more involved procedure in which charge parameters were optimized to match the calculated interaction energies of a water molecule with DMA in a variety of possible geometries. However, our approach for obtaining charge parameters has previously met with success,[39] and it has the additional advantages of simplicity and generality. Lennard-Jones parameters for DMAAN were taken from the OPLS parameter set,[37,40] using the most similar atoms available. A full description of the **Z**-matrixes and potential functions is provided in Table S1 and Scheme S1 in the Supporting Information.

A few representative complexes of DMAAN with a single water molecule were examined to verify that the potential functions would provide an adequate description of solute−solvent interactions. Table 5 compares the interaction energies obtained by using the molecular mechanical potential functions to those obtained via ab initio methods. Optimizations were carried out with no geometric constraints, initially using the HF/6-31G* level of theory chosen by Duffy et al. in their earlier study of DMA.[26] Calculations were subsequently carried out by using a recently developed procedure for predicting the strength of hydrogen-bonding interactions with density functional theory.[41] In this procedure, the Becke3LYP hybrid functional[42] is used to perform single-point calculations with

(37) Jorgensen, W. L. *BOSS, Version 3.6*; Yale University: New Haven, CT, 1996.
(38) Carlson, H. A.; Nguyen, T. B.; Orozco, M.; Jorgensen, W. L. *J. Comput. Chem.* **1993**, *14*, 1240−1249.
(39) Recent examples: (a) Fox, T.; Scanlan, T. S.; Kollman, P. A. *J. Am. Chem. Soc.* **1997**, *119*, 11571−11577. (b) Peräkylä, M.; Kollman, P. A. *J. Am. Chem. Soc.* **1997**, *119*, 1189−1196. (c) Kirchhoff, P. D.; Bass, M. B.; Hanks, B. A.; Griggs, J. M.; Collet, A.; McCammon, J. A. *J. Am. Chem. Soc.* **1996**, *118*, 3237−3246.
(40) (a) Jorgensen, W. L.; Maxwell, D. S.; Tirado-Rives, J. *J. Am. Chem. Soc.* **1996**, *118*, 11225−11236. (b) Jorgensen, W. L.; Tirado-Rives, J. *J. Am. Chem. Soc.* **1988**, *110*, 1657−1666. (c) Jorgensen, W. L.; Swenson, C. J. *J. Am. Chem. Soc.* **1985**, *107*, 569−578. (d) Jorgensen, W. L.; Swenson, C. J. *J. Am. Chem. Soc.* **1985**, *107*, 1489−1496.

Table 5. Interaction Energies of a Single Water Molecule with *N*,*N*-Dimethylaminoacrylonitrile[a]

species	interaction site	HF/6-31G* [b]	DFT[c]	BOSS[d]
ES	C≡N	−5.42	−5.67	−6.22
ES	amino N	−3.13	−2.38	−2.46
TS2	C≡N	−4.55	−4.23	−5.51
TS2	amino N	−5.22	−4.93	−4.70

[a] Energies in kcal/mol. [b] Geometries optimized at HF/6-31G*. [c] Becke3LYP/6-31++G(2d(X+),p)//Becke3LYP/6-31+G(d(X+),p), including appropriately scaled ZPE; procedure defined in: Rablen, P. R.; Lockman, J. W.; Jorgensen, W. L. *J. Phys. Chem.* **1998**, *102*, 3782−3797. [d] Derived via BOSS using TIP4P water and the CHELPG charge parameters for DMAAN; the geometries were taken from the Becke3LYP/6-31+G(d(X+),p) optimization.

Table 6. Free Energy Changes for Simulated Perturbations (298 K; kcal/mol)[a]

	perturbation			
solvent	ES → TS1	TS1 → TS2	TS2 → ES	sum
cyclohexane	+0.34 ± 0.08	+0.13 ± 0.03	−0.23 ± 0.07	+0.24 ± 0.11
acetonitrile	+2.30 ± 0.04	−0.08 ± 0.03	−2.12 ± 0.03	+0.10 ± 0.06
methanol	+2.60 ± 0.10	+0.04 ± 0.04	−2.49 ± 0.06	+0.15 ± 0.12
water	+3.27 ± 0.09	+0.00 ± 0.20	−3.10 ± 0.10	+0.17 ± 0.24

[a] The error estimates represent statistical error only, and are standard deviations derived from the statistical sampling.

Table 7. Calculated Solvent Effects on the Barrier to Rotation about the Conjugated C−N Bond in *N*,*N*-Dimethylaminoacrylonitrile Using Monte Carlo Simulations ($\Delta\Delta G^{\ddagger}$(298), kcal/mol)

	calcd			
solvent	TS1	TS2	total	exp[a]
cyclohexane	0.3	0.2	0.2	1.7[b]
acetonitrile	2.3	2.1	2.1	3.66
methanol	2.6	2.5	2.5	4.04
water	3.3	3.1	3.1	≤3.7

[a] Experimental values correspond to $\Delta\Delta G^{\ddagger}$ at 273 K, not 298 K, but the entropy component is expected to be comparatively small and the 25 °C temperature difference should introduce little error. [b] Experimental value is for methylcyclohexane.

the 6-31++G(2d(X+),p) basis set on geometries optimized by using the 6-31+G(d(X+),p)) basis set.[41] The molecular mechanical energies were computed by using fixed geometries in which the intermolecular degrees of freedom were frozen at values corresponding to those obtained from the density functional optimizations. Table 5 shows that the agreement between the different calculations is fairly good, suggesting that the molecular mechanical potential functions provide an adequate description of DMAAN.

Perturbations were then carried out between the equilibrium structure and the two transition state structures to predict the solvent effects on the bond rotation process. Simulations were carried out in TIP4P water[43] and in OPLS methanol,[44] acetonitrile,[45] and cyclohexane,[46] and the results are given in Tables 6 and 7. The three perturbations listed in Table 6 complete a thermodynamic cycle, so that the sum of the free energy changes should be zero within statistical error. In general, the cycles do yield total energies no greater than 0.25 kcal/mol, although the deviation from zero is in two cases slightly greater than the reported statistical error. Nonetheless, statistical and sampling errors appear to be well under 0.5 kcal/mol, and thus much smaller in magnitude than the phenomena under investigation. Experimental data are available for direct comparison to the simulations in water, methanol, and acetonitrile. For the cyclohexane simulations, the closest available experimental comparison is to methylcyclohexane, but no significant differences are expected between these two extremely similar solvents.

The solvent effects derived from the simulations listed in Table 6 appear in Table 7, where it can be seen that the agreement with experiment varies from good to poor. In water, the simulations predicted a solvent effect of 3.1 kcal/mol, quite close to the experimentally determined value of approximately 3.7 kcal/mol. In all other solvents, however, the simulations significantly underestimate the influence of the medium. At least in a percentage sense, the deviations are the most severe in the least polar solvents.

One of the advantages of statistical mechanical simulations is that they provide detailed structural information that can be used to elucidate the specific interactions responsible for observed macroscopic behavior. Radial distribution functions (RDF's) and pair interaction energy distributions (PIED's) represent this wealth of information in a compact and digestible manner. RDF's take the form $g_{xy}(r)$, the probability that an atom of type x will be at a distance r from an atom of type y. The RDF is typically normalized to the bulk density so that $g_{xy}(r)$ approaches a limiting value of one as the value of r increases to infinity. The PIED's constitute a frequency histogram of interaction energies between pairs of molecules (solvent−solvent or solute−solvent), organized along an axis representing the energy. The PIED thus indicates the average number of interactions present as a function of strength, e.g., a PIED might indicate 0.6 solute−solvent interactions with energies between −6.5 and −6.0 kcal/mol, 0.9 interactions between −6.0 and −5.5 kcal/mol, etc. Hydrogen bonding is generally evident in graphical representations of either RDF's or PIED's, as a distinct peak or set of peaks appearing at short internuclear distances for the former or at strong interaction energies for the latter.

RDF's for the equilibrium structure and the favored transition state of DMAAN are shown in Figures 3 and 4. The RDF's supply information about distances from the solvent OH proton to both the cyano nitrogen atom (C≡N···HO) and the amino nitrogen atom (amino R_3N···HO) of DMAAN. Figure 3 provides the data for water as the solvent, while Figure 4 provides the analogous information in methanol. The R_3N···HOH RDF appearing in Figure 3 indicates that in water, hydrogen bonding to the amino nitrogen atom is negligible in the equilibrium structure (no visible peak at short distances), while there is a small amount in the transition state structure (small peak). In methanol, hydrogen bonding to the amino nitrogen atom is negligible under all circumstances (no visible peaks). It is readily apparent, however, that the extent of hydrogen bonding to the cyano nitrogen is greater in the equilibrium structure than in the transition state structure (larger peak at short distances for the former). This change presumably contributes to the preferential stabilization of the equilibrium structure. The difference is subtle in the case of water, but quite pronounced in the case of methanol.

Quantitative measures of hydrogen bonding can be extracted from the RDF's and PIED's and used to place a discussion of specific solute−solvent interactions on firmer ground. Duffy et al. have defined as hydrogen bonding those interactions characterized by an interatomic distance less than 2.5 Å,[26] and

(41) Rablen, P. R.; Lockman, J. W.; Jorgensen, W. L. *J. Phys. Chem.* **1998**, *102*, 3782−3797.
(42) Becke, A. D. *J. Chem. Phys.* **1993**, *98*, 5648−5652.
(43) Jorgensen, W. L.; Chandrasekhar, J.; Madura, J. D.; Impey, R. W.; Klein, M. L. *J. Chem. Phys.* **1983**, *79*, 926−935.
(44) Jorgensen et al. *J. Phys. Chem.* **1986**, *90*, 1276−1284.
(45) Jorgensen, W. L.; Briggs, J. M. *Mol. Phys.* **1988**, *63*, 547−558.
(46) Jorgensen, W. L.; Madura, J. D.; Swenson, C. J. *J. Am. Chem. Soc.* **1984**, *106*, 6638−6646.

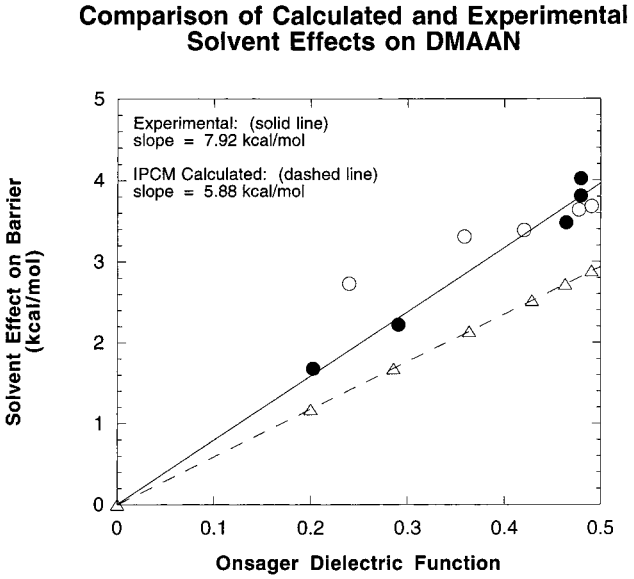

Figure 2. Comparison of experimental and IPCM calculated solvent effects on the barrier to C−N bond rotation in DMAAN. The circles represent the experimental data, while the triangles represent the calculated (IPCM) values. Only the filled circles, representing methylcyclohexane, dibutyl ether, acetone, nitromethane, and acetonitrile, were used to obtain the solid least-squares line representing the experimental relationship. The IPCM data points and the corresponding dashed line represent predictions from the MP2/6-311++G** level of theory. Experimental best fit line: solvent effect (kcal/mol) = $7.92*(\epsilon - 1)/(2\epsilon + 1) + 0.01$; $r^2 = 0.98$. IPCM best fit line: solvent effect (kcal/mol) = $5.88*(\epsilon - 1)/(2\epsilon + 1)$; $r^2 = 1.00$.

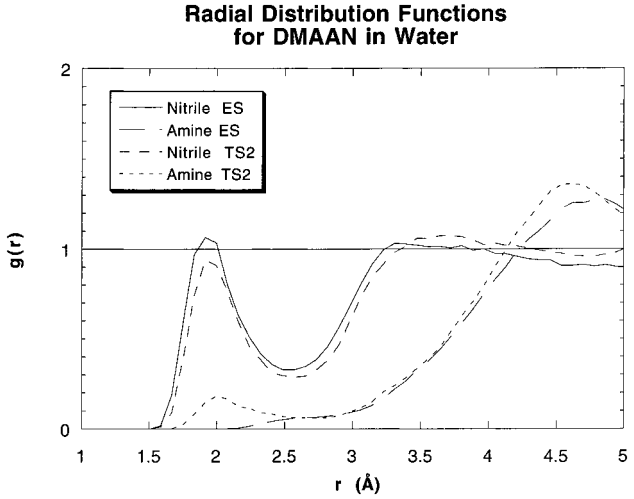

Figure 3. Computed radial distribution functions for DMAAN in water. The reference point in the water molecule is the proton.

we have taken the same approach here. Integration of the appropriate RDF from zero to 2.5 Å provides the average number of hydrogen bonds of the type described by the RDF. In this manner, the numbers of hydrogen bonds from water and methanol to both the cyano and amino nitrogen atoms of DMAAN were computed for the equilibrium structure and both transition states. The results are listed in columns 3 and 5 of Table 8.

Estimation of average hydrogen bond energies is also possible, through integration of appropriate portions of the PIED. Integration begins with the strongest interactions observed, and continues along the energy axis of the PIED until the total *number* of interactions integrated equals the total number of hydrogen bonds obtained earlier from the RDF. Under the assumption that the strongest interactions are also the ones with the shortest distances in the RDF, this procedure yields an approximate measure of the average and total hydrogen bond *strengths*, and these are listed in columns 8 and 9 of Table 8. Finally, the hydrogen bond energy was approximately decomposed into contributions from the amino and cyano hydrogen bonds, and the results are listed in parentheses in Table 8. The decomposition was accomplished algebraically by assuming that (1) average hydrogen bond strengths were the same for the two transition states and (2) the difference in average hydrogen bond strength between the equilibrium structure and the transition state was equal to the corresponding difference in the interaction energies of a single water molecule with either the equilibrium structure or the transition state of DMAAN in the gas phase (i.e., the rightmost column of Table 5). These assumptions are only approximate, and so the decomposition of the energy into components corresponding to the two individual hydrogen bonds must be regarded as merely qualitative.

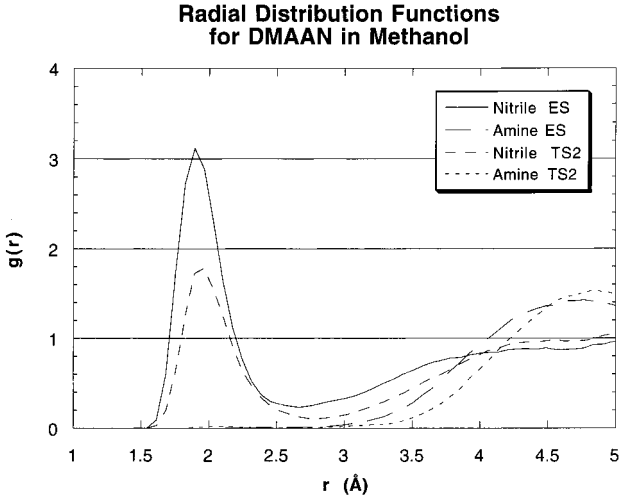

Figure 4. Computed radial distribution functions for DMAAN in methanol. The reference point in the methanol molecule is the alcohol proton.

Table 8. Analysis of Radial Distribution Functions[a]

		H-bond to C≡N		H-bond to amine		total		
species	solvent	av no.[b]	av E^c	av no.[d]	av E^c	av no.[e]	av E^f	tot E^g
ES	H_2O	0.567	(−5.98)	0.012	(−0.94)	0.579	−5.88	−3.40
TS1	H_2O	0.473	(−5.27)	0.109	(−3.18)	0.582	−4.88	−2.84
TS2	H_2O	0.483	(−5.27)	0.089	(−3.18)	0.572	−4.94	−2.82
ES	MeOH	1.269		0.009		1.278	−5.19	−6.59
TS1	MeOH	0.759		0.001		0.760	−4.38	−3.33
TS2	MeOH	0.770		0.009		0.779	−4.48	−3.49

[a] Obtained from Monte Carlo simulations of DMAAN in TIP4P water and OPLS methanol; energies in kcal/mol. [b] Average number of hydrogen bonds from water to the cyano nitrogen, obtained by integration of the C≡N···HOH radial distribution function from 0 to 2.5 Å, as described in the text. [c] Estimated using the numbers of hydrogen bonds to the cyano and amino nitrogens, the total solute−solvent hydrogen bond energy, and energy differences from Table 5, as described in the text. [d] Average number of hydrogen bonds from water to the amino nitrogen, obtained by integration of the amino N···HOH radial distribution function from 0 to 2.5 Å, as described in the text. [e] Sum of the number of hydrogen bonds to the cyano nitrogen (column 3) and to the amino nitrogen (column 5). [f] Total hydrogen bond energy (column 9) divided by the total average number of hydrogen bonds (column 7). [g] Derived by integration of the energy pair distribution as described in the text.

(47) (a) Perng, B.-C.; Newton, M. D.; Raineri, F. O.; Friedman, H. L. *J. Chem. Phys.* **1996**, *104*, 7153−7176. (b) Perng, B.-C.; Newton, M. D.; Raineri, F. O.; Friedman, H. L. *J. Chem. Phys.* **1996**, *104*, 7177−7204.

Discussion

Self-Consistent Reaction Field Calculations. Previously it has been shown that the barriers to rotation in DMA and DMF are reproduced remarkably well by self-consistent reaction field calculations, at least for solvents which are not hydrogen bond donors, are not aromatic, and are not halogenated.[22] The lack of agreement for hydrogen bond donating solvents is not surprising, given that the model neglects the details of hydrogen bonding. The physical basis for the exclusion of protic solvents is thus clearly defined. The deviations for aromatic and chlorinated solvents are less easily understood, but might result from short-range interactions with polar solutes that are stronger than expected on the basis of the dielectric constant. As discussed briefly in the preceding paper, either high electronic polarizability or a large quadrupole moment could lead to strong short-range interactions that would affect microscopic behavior significantly but influence the bulk dielectric constant only weakly.[30,47]

The Onsager model that lies at the heart of self-consistent reaction field theory predicts a linear relationship between the barrier and the dielectric function, $(\epsilon - 1)/(2\epsilon + 1)$. Examination of Table 3 and Figure 2 shows that for methylcyclohexane, dibutyl ether, acetone, acetonitrile, and nitromethane (filled circles), the experimentally determined barriers obey this relationship closely.[48] These are the solvents for which a linear dependence is expected, based on the known behavior of DMA and DMF.[22] However, the slope of this linear relationship is 7.9 kcal/mol experimentally, while the IPCM calculations predict a slope of 5.5 kcal/mol at the HF/6-31G* level or of 5.9 kcal/mol at the MP2/6-311++G** level. The difference in the slopes of the calculated and experimental least-squares lines is clearly evident from visual inspection of Figure 2. Thus, the IPCM model underestimates the magnitude of the solvent effect in DMAAN by 30% even in the "well-behaved" solvents. The IPCM model also underestimates the solvent effects in DMF and DMA, but only by about 10%.[22] Interestingly, the protic solvents water and methanol fall on the same line as the aprotic solvents, and so the IPCM model appears to reproduce medium effects more or less correctly even in protic solvents. However, this success with protic solvents cannot be of a general nature, as the neglect of explicit hydrogen-bonding interactions is know to be problematic for the case of amides.[22,26] Instead it must follow from the apparent lack of a specific hydrogen-bonding component to the solvent effects in this system.

The lack of quantitative accuracy of the model might conceivably be ameliorated by choosing a different value for the electron density contour. The IPCM model defines the solute−solvent boundary as the isosurface characterized by a particular value for the gas-phase calculated electron density of the solute, and the value 0.0004 electrons per cubic Bohr contour was initially chosen for this purpose, consistent with previous recommendation.[19] Nonetheless, the isodensity contour is an empirical parameter, and the underestimate of the observed solvent effect might result from the use of too small a value, i.e., defining too large a cavity. The results in Table 4, however, demonstrate that increasing the isodensity contour to 0.001 or even 0.002 increases the predicted solvent effect by no more than 10%. The relative insensitivity of the model to the isodensity value is consistent with the earlier findings of Wiberg et al.[19] The inability of the model to reproduce the full magnitude of the solvent effect thus cannot result primarily from an inappropriate choice of the isodensity contour value, and must instead reflect a deeper problem. Nonetheless, the results of this study suggest that 0.001 electrons per cubic Bohr might be slightly more appropriate than 0.0004 for the isodensity contour in the IPCM and SCIPCM models.[49]

Statistical Mechanical Simulations. In the case of DMA, statistical mechanical simulations were able to reproduce the *difference* in solvent effect between water and carbon tetrachloride fairly well,[26] although the values of the solvent effects with respect to the gas phase were significantly underestimated. With DMAAN, the behavior of the simulations is quite different. The calculated solvent effect in water is fairly close to correct, at 3.1 kcal/mol, compared to the experimental value of 3.7 kcal/mol. Furthermore, the experimental value is subject to some uncertainty, due to both the inadequately defined line shape in the solution experiment and the lack of a true gas-phase experimental value. The agreement between theory and experiment thus appears to be satisfactory. Water is in fact the solvent in which one would most expect these sorts of simulations to yield accurate results, as it is for aqueous solutions that the simulation methodology has been most thoroughly refined.

For the other solvents, however, the statistical mechanical simulations consistently underestimate the solvent effect by approximately 1.5 kcal/mol. It is known that classical mechanical simulations that use fixed charge parameters can only account for solvent electronic polarization in an "averaged" sense. In water, which is already highly polarized in the pure liquid state for which the solvent charge parameters are optimized, this approximation seems to work quite well. In nonpolar solvents, however, the pure liquid state is characterized by very little or no polarization, even though such polarization is possible in the presence of a polar solute. Consequently, the use of fixed charges all but guarantees that the calculations will seriously underestimate solvation energies in nonpolar solvents. It has been shown that the inclusion of an approximate polarization component in the solute−solvent potential functions of cyclohexane can correct this error.[50] The current observation that the simulations significantly underestimate the solvent effect in cyclohexane is thus consistent with the expected importance of solvent polarization.

The cases of acetonitrile and methanol are somewhat more puzzling. One might have expected the error in acetonitrile to be intermediate between that in methanol and that in cyclohexane. However, in fact the calculations fall short of experiment by almost exactly the same amount in all three cases, and the reasons for the discrepancies are not clear. It is worthy of note, however, that the solvent effect in acetonitrile exceeds not only the Monte Carlo prediction but also the prediction derived from the empirical correlation with the Onsager dielectric function. The solvent effect in acetonitrile thus appears to be consistently higher than expected. This behavior might result from acetonitrile's high degree of electronic polarizability, which might in turn lead to stronger than expected short-range solute−solvent interactions.[30] Speculation about why the simulations in metha-

(48) It is worthy of note that the data point for acetonitrile in Figure 2 lies somewhat above the best fit line, indicating a higher barrier than in other solvents having comparable values for the Onsager dielectric function. This deviation possibly indicates that acetonitrile, like the aromatic and chlorinated solvents, yields somewhat stronger than expected interactions with polar solutes due to unusually great electronic polarizability. The "soft" π-system of acetonitrile could certainly account for such polarizability. A similar pattern was observed with DMA and DMF previously, where again acetonitrile yielded a somewhat stronger solvent effect than did acetone.

(49) The default value for this parameter in the Gaussian 94 code is in fact 0.001 electrons per cubic Bohr, not 0.0004. Use of the larger contour would probably also improve the calculated results for DMA.

(50) Jorgensen, W. L.; McDonald, N. A.; Selmi, M.; Rablen, P. R. *J. Am. Chem. Soc.* **1995**, *117*, 11809−11810.

nol do not properly reproduce the full magnitude of the observed solvent effect is offered in a subsequent paragraph.

The Absence of an Apparent Hydrogen-Bonding Component to the Solvent Effect. Both DMF and DMA have significantly higher rotational barriers in water and methanol than in aprotic solvents of comparable dielectric function.[22] In their Monte Carlo study of DMA in water, Duffy et al. provided a decomposition of the solute−solvent hydrogen-bonding interactions similar to that presented for DMAAN in Table 8.[26] They attributed the preferential stabilization of the equilibrium structure of DMA to a reduced number and strength of hydrogen bonds in the transition state. During the process of rotating from the mimimum to the transition state, the number of hydrogen bonds to the carbonyl was observed to decrease by 33%, and the average strength of these bonds by 6%, for an overall decrease of 40% in the associated stabilization. There was also a slight increase in hydrogen bonding to the nitrogen, but the energetic consequences of hydrogen bonding at the carbonyl were clearly dominant.

Table 8 shows that for DMAAN, a somewhat similar pattern emerges. On going from the minimum to the transition state in water, the number of hydrogen bonds to the nitrile decreases by 15%, and the average strength decreases by 12%, for an overall decrease of 25% in the associated stabilization. Again, there is a compensating increase in the number and strength of hydrogen bonds to the amino nitrogen atom, but the energies involved are much smaller than for hydrogen bonding at the nitrile. Why, then, is there a distinct hydrogen-bonding effect on the barrier for DMA, but not for DMAAN? The answer appears to be mostly that hydrogen bonding is simply much less extensive to DMAAN than to DMA. According to the simulations, the cyano nitrogen of DMAAN has an average of about 0.57 hydrogen bonds, while the carbonyl oxygen of DMA has an average of about 1.55. This observation is in accord with the greater basicity of amides relative to nitriles,[41] and with calculations in the preceding paper showing specifically that DMAAN is 4.3 kcal/mol less basic than DMA in the gas phase.[30] If only about one-third as much hydrogen bonding occurs to the nitrile as to the amide, as indicated by the RDF's, then one might expect the specific effect of protic solvents to be only one-third as great for DMAAN as for DMA. Hydrogen bonds to the nitrile nitrogen of DMAAN are on average slightly stronger (6.0 kcal/mol) than those to the carbonyl oxygen of DMA (4.5 kcal/mol), but clearly the difference in the *number* of interactions will be dominant here.

In addition, the hydrogen bond analyses suggest that the extent of hydrogen bonding in DMA decreases more steeply (33%) on going to the transition state than does hydrogen bonding in DMAAN (15%). A steric explanation can account for a portion of this difference. In the preferred anti transition state of DMA, the *N*-methyl groups are situated quite close to the carbonyl oxygen, in such a way that hydrogen bond donation by water to the carbonyl is probably inhibited. In accord with this hypothesis, Duffy et al. predicted that the alternative syn transition state, in which such steric interference would be absent, has just as much hydrogen bonding to the carbonyl oxygen as does the equilibrium structure. With DMAAN, on the other hand, the rotating dimethylamino group is located quite distant from the cyano nitrogen atom, and as a result rotation from the minimum to the transition state has little steric consequence for solvation at the nitrile. However, electronic factors probably also play a role. Difference density calculations show that only about 20% as much π-electronic reorganization occurs at the cyano nitrogen of DMAAN (0.016 electrons)[30] as occurs at the carbonyl oxygen of an amide (0.088 electrons)[51] during the analogous bond rotation processes. This difference in behavior is expected to make bond rotation in DMA more sensitive to hydrogen bonding than bond rotation in DMAAN.

It is readily apparent from Figure 3 and Table 8 that in water, hydrogen bonding to the amino nitrogen is negligible for the equilibrium structure, while there is a small amount for the transition state. In methanol, hydrogen bonding to the amino nitrogen atom is negligible under all circumstances. The number and strength of hydrogen bonds to the cyano nitrogen atom, on the other hand, changes significantly between the equilibrium structure and the transition state. In water, both the number and strength of hydrogen bonds are greater for the equilibrium structure, amounting to a total difference in solute−solvent hydrogen-bonding energy of 0.8 kcal/mol. In methanol, the predicted difference is much more pronounced, primarily because of a very large change in the predicted *number* of interactions, such that the predicted solute−solvent hydrogen-bonding energy is 3.1 kcal/mol greater in the equilibrium structure than in the favored transition state.

The simulations thus offer a clear explanation of the behavior observed in water. The behavior in methanol, however, is more difficult to understand. The simulations predict a relatively small solvent effect in methanol, significantly lower than what is observed. The hydrogen bond analysis in Table 8, on the other hand, as well as the RDF's in Figure 3, clearly suggests that hydrogen bonding to the nitrile nitrogen is substantially greater in methanol than in water. Integration of the RDF yields an average of 1.27 hydrogen bonds to the nitrile for the equilibrium structure of DMAAN (compared to 0.57 in water), and a precipitous decrease to 0.77 for the transition state. On the basis of this observation, one would expect a substantial increase in the rotational barrier in methanol, but such an increase is neither predicted by the free-energy perturbations nor observed experimentally. Evidently, changes in solvent−solvent interactions and/or long-range solute−solvent interactions more than compensate for the changes in solute−solvent hydrogen bonding.

Equilibrium Treatment of the Transition State. Both models used here to describe the influence of solvents on bond rotation in DMAAN significantly underestimate the magnitude of the effect. The statistical mechanical simulations in water come the closest to yielding the experimentally derived results; in all other cases, theory underestimates the solvent effect by 1.0−2.0 kcal/mol, with the largest errors generally occurring in polar aprotic solvents. One might speculate that the problem derives from the lag between solute conformational change and the corresponding reorientation of solvent molecules.

Although the rate of amide bond rotation is in some sense "slow", "slow" in this context means that any given molecule only has a small chance of undergoing isomerization during a given amount of time. However, when a given molecule does isomerize, the nuclear motions are in fact very fast. Consequently, the solvation of the transition state is not characterized by a condition in which the arrangement of solvent molecules is fully equilibrated.[52−55] Although enough time is available for electronic reorganization to occur, there is not enough time for extensive nuclear reorganization of the solvent molecules to take place. The solvent molecules instead must remain in more or

(51) Wiberg, K. B.; Rablen, P. R. *J. Am. Chem. Soc.* **1995**, *117*, 2201−2209.
(52) Waldeck, D. H. *J. Mol. Liq.* **1993**, *57*, 127−148.
(53) Waldeck, D. H. *Chem. Rev.* **1991**, *91*, 415−436.
(54) Park, N. S.; Waldeck, D. H. *J. Phys. Chem.* **1990**, *94*, 662−669.
(55) Zeglinski, D. M.; Waldeck, D. H. *J. Phys. Chem.* **1988**, *92*, 692−701.

less the same arrangement over the entire course of the bond rotation process of the solute. Consequently the equilibrium treatment of solvation that is appropriate for the minimum is not equally appropriate for the transition state structure.[52−55]

Nonetheless, both models of solvation studied here assume equilibration of the solvent. In Monte Carlo simulations, equilibration is literally carried out prior to thermodynamic averaging. In continuum calculations, the use of the static dielectric constant implies equilibration. The dielectric constant is frequency dependent, and for almost all organic solvents has a value of only about 2.0 in the optical frequency range. At optical frequencies, motion of electrons in response to an oscillating electric field is possible (electronic polarization), but motion of nuclei is not. As the process of equilibration ought, in general, to reduce the total free energy, equilibrated treatment of the transition state should always lead to a solvation energy for the transition state that is too favorable. That in turn leads to an underestimate of the barrier to rotation, and thus in the present case to an underestimate of the solvent effect on bond rotation. This sort of dynamical effect *always* decreases the actual rate of reaction compared to that predicted on the basis of equilibrium solvation, and so is frequently considered formally to be a frictional effect.[53] From this point of view, the decrease in the rate constant is associated with the preexponential term in the Arrhenius or Eyring expression, even though in reality the separation from barrier height is by no means rigorous.[53] The component of friction resulting from the sluggishness of reorientation of polar solvent molecules is often termed dielectric friction.[53,56]

If nonequilibrium solvation effects, and dielectric friction in particular, are primarily to blame for the underestimate of solvent effects on bond rotation rates, then one might expect the seriousness of the underestimate to depend on the degree to which the orientation of the molecular dipole moment of the solute changes upon going from the minimum to the transition state. If the orientation changes only slightly, little solvent reorganization would be necessary to achieve equilibration, and so inappropriate inclusion of equilibration should lead to only a small error. If the orientation changes substantially, however, equilibration would require a greater reorganization of the solvent, and so nonequilibrium effects would be expected to play a more significant role.

With this thinking in mind calculations were carried out to determine the change in orientation of the dipole moment for DMA and DMAAN, and the results are listed in Table 9. With DMA, the dipole moment is substantially smaller for the preferred anti transition state structure (TS1) than it is for the equilibrium structure. However, the orientation of the dipole moment barely changes at all (5°). Thus one might expect nonequilibrium solvation effects (dielectric friction) to play a minor role, in agreement with the observation that the solvent effects in this system are fairly well reproduced by simple solvation models. With DMAAN, on the other hand, the orientation of the dipole moment changes by a more substantial 26° on going from the equilibrium structure to the favored transition state structure (TS2). Consequently, nonequilibrium effects might be expected to play a more important role in this system. This hypothesis is in accord with the more substantial underestimation (30%) of the solvent effect for DMAAN with use of the same IPCM continuum model that underestimated the effect in DMA by only 10%. It also is consistent with the observation that statistical mechanical simulations seem to underestimate solvent effects more seriously for DMAAN than for DMA.

Table 9. Calculated Dipole Moments for the Equilibrium Structure and the Transition State Structures of *N,N*-Dimethylacetamide and *N,N*-Dimethylaminoacrylonitrile (MP2/6-311++G**//MP2/6-31G*)

	dipole moment[a]				change[b]	
species	*X*	*Y*	*Z*	total	Δr	$\Delta\theta$
DMA, ES	0.978	0.269	3.780	3.914		
DMA, TS1	0.343	0.000	1.725	1.759	2.168	5.1
DMA, TS2	−0.627	0.000	3.513	3.569	1.649	24.9
DMAAN, ES	0.724	1.343	6.478	6.655		
DMAAN, TS1	0.494	0.000	4.194	4.223	2.660	11.7
DMAAN, TS2	−1.350	0.000	4.272	4.480	3.312	26.4

[a] *X*, *Y*, and *Z* components and total magnitude of the calculated dipole moment (debye units). The orientation of the molecule was defined with the C=O bond along the *z*-axis and the nitrogen in the *xz*-plane (DMA) or the C_1-C_2 bond along the *z*-axis and C_3 in the *xz*-plane (DMAAN). [b] Change in dipole moment magnitude and orientation upon going from the equilibrium structure to the transtion state structure.

As a final remark, it is noteworthy that the statistical simulations reproduce the increase in barrier height in water relative to the gas phase moderately well (predicted solvent effect of 3.1 kcal/mol, actual solvent effect approximately 3.7 kcal/mol), but describe the situation in methanol significantly less accurately (predicted solvent effect of 2.5 kcal/mol, experimental value 4.0 kcal/mol). If a substantial portion of the underestimate of the solvent effects is attributed to dynamical effects (i.e., solvent friction), then indeed one would expect the error to be more serious in methanol than in water due to the much more sluggish response time of the latter solvent. For instance, whereas the dielectric relaxation time constant for water was been measured as 0.54 ps, the corresponding measurement for methanol gives a relaxation time constant of 9.2 ps.[57]

Comparison of the Models. Both the IPCM model and statistical mechanical simulations suffer from a consistent shortfall of at least 1−2 kcal/mol in the predicted solvent effect on bond rotation in DMAAN.[58] At least a portion of this inadequacy probably results from a dynamical effect that will similarly influence almost any reasonably simple solvation model. If all the predicted solvent effects are arbitrarily increased by ∼30% to compensate for this shortcoming, then one can assert that the IPCM calculations yield good agreement with experiment in the aprotic, nonhalogenated, nonaromatic solvents for which the model has performed well previously. From this perspective the Monte Carlo simulations in water also yield good agreement with experiment, although the simulations in other solvents are less satisfactory. The lack of a significant predicted solvent effect in cyclohexane results from the neglect of solvent electronic polarization induced by the solute, and is well understood. The same factor might also contribute to the underestimate of solvent effects in acetonitrile. The discrepancy between theory and experiment in methanol is more difficult to understand, but quite possibly results from an exaggerated dielectric frictional effect that is enhanced by the unusually slow relaxation times characteristic of alcohols. It is also of course possible that the atomic charges used for DMAAN are not optimal, and that agreement with experiment could be somewhat improved by fitting them so as to reproduce not the molecular

(56) (a) Alavi, D. S.; Waldeck, D. H. *J. Chem. Phys.* **1991**, *94*, 6196−6202. (b) Alavi, D. S.; Hartman, R. S.; Waldeck, D. H. *J. Chem. Phys.* **1991**, *94*, 4509−4520.

(57) Marconcelli, M.; MacInnis, J.; Fleming, G. R. *Science* **1989**, *243*, 1674−1681.

(58) The one partial exception to this statement is the set of Monte Carlo simulations in TIP4P water, where the experimentally determined solvent effect is underestimated by only about 0.6 kcal/mol.

electrostatic potential but rather a set of interaction energies with a single water molecule, as in the approach of Duffy et al.[26]

Setting aside the frictional effects, which will be difficult to handle in any model, the following patterns emerge from the combined results for DMAAN and DMA. For aprotic, nonhalogenated, nonaromatic solvents, reaction field calculations of the sort implemented in the IPCM model offer a simple and fairly inexpensive method for reliably predicting solvent effects. Furthermore, given the pattern in which halogenated and aromatic solvents *consistently* yield larger solvent effects than predicted by the model, it is likely that these solution environments could be adequately treated also, simply by using an enhanced "effective" dielectric constant. For water, on the other hand, statistical mechanical simulations yield good accuracy, while the IPCM calculations not surprisingly yield more or less unpredictable results. This agreement between theory and experiment would probably extend to other protic solvents as well, so long as frictional effects are not exaggerated, as they apparently are in methanol. Such frictional factors are, of course, irrelevant for equilibrium solvent effects. On the other hand, simulations are neither economical nor reliable for treating nonpolar solvents where solute-induced electronic polarization is of paramount importance.[59]

Summary

A quantum mechanical continuum solvation model (IPCM) reproduces the experimentally observed solvent effects on bond rotation in DMAAN with some success. The model has previously been found to describe adequately aprotic solvents that lack aromatic rings and second-row atoms. For methylcyclohexane, dibutyl ether, acetone, nitromethane, and acetonitrile, the IPCM calculations predict the solvent effects in a qualitatively correct fashion. The experimental data correlate closely with the Onsager dielectric function, $(\epsilon - 1)/(2\epsilon + 1)$, and the best fit line is characterized by the expected positive slope. However, the model underestimates the magnitude of the slope by 30%. These findings diverge from the corresponding results for amides, where the model yields predictions within 10% of experiment. Changing the isodensity contour value in the IPCM calculations from 0.0004 to 0.001 electrons per cubic Bohr improves the agreement with experiment, but only slightly. It is postulated that the larger than predicted barriers in polar solvents arise from solvent dielectric friction. This term is used to describe the additional resistance to isomerization that results from treating the solvation of the transition state in an equilibrium manner, even though the transition state does not exist sufficiently long for the solvent structure to equilibrate.

Monte Carlo statistical mechanical simulations reproduced the experimentally observed solvent effects in water, methanol, acetonitrile, and cyclohexane in a qualitatively correct fashion, but achieved quantitative accurately only in the case of water. The failure of statistical mechanical models to account for solvent effects in nonpolar solvents such as cyclohexane has been previously documented and is well understood to result from the inability of the traditional pairwise additive potential functions to account for electronic polarization of the solvent.[50] The underestimate of the solvent effect in acetonitrile is of the same magnitude in an absolute sense, but is much smaller in a proportional sense, as expected. Some of the problem might again result from omission of solute−solvent polarization. It is worthy of note that the IPCM calculations also were unable to reproduce the full solvent effect in acetonitrile. In methanol, on the other hand, the serious underestimate of the solvent effect is attributed to dynamical effects, which should be particularly pronounced in methanol, which is characterized by especially slow solvent reorganization.

In water, the Monte Carlo simulations only underestimate the solvent effect by 20%, and thus provide the most accurate result obtained from either model. The residual error likely results from the same nonequilibrium effects that cause the IPCM calculations to be consistently 30% too low, although it is also possible that the CHELPG-derived potential functions for DMAAN are not optimal. The simulations suggest that there are two reasons why hydrogen bonding by the solvent does not markedly increase the barrier to rotation in DMAAN the way it does in DMA. First, hydrogen bonding to the nitrile group of DMAAN is much less extensive than hydrogen bonding to an amide carbonyl, such that the former has on average only about one-third as many hydrogen bonds in aqueous solution as does the latter. This tendency is in accord with the greater basicity of the nitrile nitrogen of DMAAN relative to the carbonyl oxygen of DMA. Second, the number of hydrogen bonds decreases more precipitously for DMA than for DMAAN as C−N bond rotation occurs. The more pronounced decrease in the case of DMA probably results largely from steric interference of carbonyl solvation by the nearby *N*-methyl groups, which does not occur in DMAAN due to the longer distance between the rotating dimethylamino group and the nitrile functional group. However, the more extensive electronic reorganization occurring at the carbonyl oxygen atom of amides relative to the cyano nitrogen of DMAAN during the analogous bond rotation processes also probably plays some role.

Calculations

Ab Initio Calculations. The Gaussian 94 package[60] was used to carry out all ab initio calculations. Standard Pople-type basis sets with six Cartesian d functions were employed.[61] The nature of all stationary points in the gas phase was verified by calculation of the HF/6-31G* vibrational frequencies. The IPCM calculations were conducted with the contour set at 0.0004 electrons per cubic Bohr unless otherwise noted. To demonstrate the linear dependence of the predicted solvent effect upon the Onsager dielectric function, a series of calculations were carried out at the HF/6-31G* level with the dielectric constant ϵ set to 2.0, 3.0, 5.0, 10.0, 20.0, and 78.0. The gas-phase HF/6-31G* optimized geometries were used for these calculations. Further IPCM calculations were conducted at MP2/6-31G*, MP2/6-311++G**, Becke3LYP/6-31G*, and Becke3LYP/6-311++G**.[60] The MP2 calculations made use of the gas-phase MP2/6-31G* optimized geometries, while the density functional calculations made use of the gas-phase HF/6-31G* optimized geometries. Density functional calculations[62] employed the Becke3LYP keyword, which invokes Becke's 3-parameter hybrid method[42] using the correlation functional of Lee, Yang, and Parr.[63,64] Density = current was specified for MP2 calculations to ensure use of

(59) If electronic polarization terms are explicitly incorporated into the potential functions, then it is of course possible to treat nonpolar solvents correctly, but the cost in computer time is generally very high.

(60) Frisch, M. J.; Trucks, G. W.; Schlegel, H. B.; Gill, P. M. W.; Johnson, B. G.; Robb, M. A.; Cheeseman, J. R.; Keith, T.; Petersson, G. A.; Montgomery, J. A.; Raghavachari, K.; Al-Laham, M. A.; Zakrzewski, V. G.; Ortiz, J. V.; Foresman, J. B.; Cioslowski, J.; Stefanov, B. B.; Nanayakkara, A.; Challacombe, M.; Peng, C. Y.; Ayala, P. Y.; Chen, W.; Wong, M. W.; Andres, J. L.; Replogle, E. S.; Gomperts, R.; Gonzalez, C.; Martin, R. L.; Fox, D. J.; Binkley, J. S.; Defrees, D. J.; Baker, J.; Stewart, J. P.; Head-Gordon, M.; Gonzalez, C.; Pople, J. A. *Gaussian 94* (Revision C.2); Gaussian, Inc., Pittsburgh, PA, 1995.

(61) Hehre, W. J.; Radom, L.; Schleyer, P. v. R.; Pople, J. A. *Ab Initio Molecular Orbital Theory*; Wiley: New York, 1986.

(62) Parr, R. G.; Yang, W. *Density Functional Theory of Atoms and Molecules*; Oxford University Press: New York, 1989.

(63) Lee, C.; Yang, W.; Parr, R. G. *Phys. Rev. B* **1988**, *37*, 785−789.

(64) Miehlich, B.; Savin, A.; Stoll, H.; Preuss, H. *Chem. Phys. Lett.* **1989**, *157*, 200−206.

the correlated charge density distribution for determination of molecular dipole moments.

Monte Carlo Simulations. Rigid geometries derived via ab initio MP2/6-31+G* optimization were used to describe the equilibrium structure and the two transition state structures of DMAAN.[60] Atomic charges were obtained via the CHELPG[65] procedure at the HF/6-31G* level as described in the Results section. The potential functions used to describe DMAAN are listed in complete detail in Table S1 and Scheme S1 in the Supporting Information. No intramolecular energy terms were included. The **Z**-matrixes for the free energy perturbations also appear in the Supporting Information.

A preequilibrated box containing 267 solvent molecules was used for each free energy perturbation simulation. The solvent−solvent nonbonded cutoff (RCUT) was set to 8.5 Å, and the solute−solvent cutoff (SCUT) to 9.5 Å. Simulations were carried out in the NPT ensemble at 1.00 atm and at 25 °C. Preferential sampling was employed, with the WKC parameter set to 150. TIP4P water,[43] methanol,[44] and acetonitrile[45] were used as defined by the OPLS potential functions[40] and supplied directly in the BOSS package.[37] A rigid united-atom cyclohexane solvent model was defined by using the custom solvent feature and the OPLS potential functions.[46] Perturbations were carried out with use of double-wide sampling, in 11 approximately equally spaced windows for water, methanol, and cyclohexane, and in 21 windows for acetonitrile. The exact reaction coordinates are provided in Tables S2 and S3 in the Supporting Information. For each window, equilibration was carried out for 7.5 million configurations, followed by at least 18 million configurations of averaging. The reported uncertainties were derived from fluctuations over separately averaged runs of 500 000 configurations. Procedures for free energy perturbations with conformational isomerization reactions have been described in detail previously.[26,66]

Acknowledgment. Financial support for this work was provided by a Faculty Start-up Grant for Undergraduate Institutions from the Camille and Henry Dreyfus Foundation, by a Cottrell College Science Award of Research Corporation, and by Swarthmore College. Acknowledgment is also made to the donors of the Petroleum Research Fund, administered by the American Chemical Society, for partial support of this research. We thank Kenneth Wiberg of Yale University for helpful discussions and preliminary review of the manuscript.

Supporting Information Available: Ab initio calculated energies in hartrees, calculated molecular geometries in **Z**-matrix form, listing of potential function parameters (atomic charges and Lennard-Jones factors) used for statistical mechanical simulations, and **Z**-matrices used for free energy perturbations (PDF). See any current masthead page for Web access instructions.

JA9823058

(65) (a) Breneman, C. M.; Wiberg, K. B. *J. Comput. Chem.* **11**, *1990*, 361. (b) Chirlian, L. E.; Francl, M. M. *J. Comput. Chem.* **1987**, *8*, 894.

(66) Jorgensen, W. L.; Buckner, J. K. *J. Phys. Chem.* **1987**, *91*, 6083−6085. Jorgensen, W. L.; Gao, J. *J. Am. Chem. Soc.* **1988**, *110*, 4212−4216.